

Article

Hydrodynamic Behaviors and Geochemical Evolution of Groundwater for Irrigation in Yaoba Oasis, China

Ting Lu ^{1,2}, Aidi Huo ^{1,2,3,*} , Jucui Wang ^{1,2}, Yudong Lu ^{1,2}  and Weibo Zhou ¹

¹ Key Laboratory of Subsurface Hydrology and Ecological Effects in Arid Region of the Ministry of Education, Chang'an University, Xi'an 710054, China

² School of Water and Environment, Chang'an University, Xi'an 710054, China

³ Xi'an Monitoring, Modelling and Early Warning of Watershed Spatial Hydrology International Science and Technology Cooperation Base, Chang'an University, Xi'an 710054, China

* Correspondence: huoaidi@chd.edu.cn

Abstract: The Yaoba Oasis is an irrigated cropland entirely dependent on groundwater; previous investigations (1980–2015) revealed an over-abstraction of groundwater and deteriorating groundwater quality. For further exploring the hydrodynamic behaviors and geochemical processes of groundwater during the irrigation season, groundwater samples were collected and analyzed using different techniques including classical statistics, correlation analysis, Piper diagrams, and Gibbs diagrams. The results indicated that Na⁺, K⁺, SO₄²⁻ and Cl⁻ were the main ions in groundwater, which were significantly correlated with TDS. The water–rock interaction is manifested by the precipitation of calcite and dolomite and the dissolution of rock salt and gypsum as an increase in TDS related to evaporation. In addition, the increasing complexity of hydrochemical type is caused by the rapid variation of hydrodynamic regime, irrigation and evaporation, which are subjected to the constraints of salty water intrusion from the desert salty lake and infiltration of irrigation return flow. Existing wells should limit overexploitation to halt the decline in groundwater levels and cut down irrigation water to reduce the risk of groundwater contamination and restore ecological balance in desert oasis.

Keywords: desert oasis; groundwater chemistry; evolution law; salty water intrusion; irrigation return flow



Citation: Lu, T.; Huo, A.; Wang, J.; Lu, Y.; Zhou, W. Hydrodynamic Behaviors and Geochemical Evolution of Groundwater for Irrigation in Yaoba Oasis, China. *Water* **2022**, *14*, 3924. <https://doi.org/10.3390/w14233924>

Academic Editor: Dimitrios E. Alexakis

Received: 25 October 2022
Accepted: 28 November 2022
Published: 2 December 2022

Publisher's Note: MDPI stays neutral with regard to jurisdictional claims in published maps and institutional affiliations.



Copyright: © 2022 by the authors. Licensee MDPI, Basel, Switzerland. This article is an open access article distributed under the terms and conditions of the Creative Commons Attribution (CC BY) license (<https://creativecommons.org/licenses/by/4.0/>).

1. Introduction

An oasis is considered one of the cradles of civilization that has significantly contributed to social progress and sustainable development. Some oases distributed worldwide include those in Amu Darya in Central Asia, Isfahan Oasis and oases in the Syr Darya River Basin in Western Asia, desert oases in the American West, desert oases in Australia, and desert oases in the piedmont areas of Qilian Mountains, Tianshan Mountains, Kunlun Mountains, Helan Mountains, and Yinshan Mountains in Northwestern China, among others [1]. Groundwater resources are an integral part of the water system that sustains life on Earth. Stable water flow and high water quality provide an important guarantee for the industrial and agricultural development of oases in arid regions [2,3]. Oases sit in the transition between arid and semi-arid regions with desert and semi-desert climates, and they are usually supported by a stable water source supply. These landscapes combine the optimal climate, hydrology, geology, and geomorphology [4,5] for the reproduction of plants and animals and for different human activities. In arid regions, about 90% of the population and over 85% of the social wealth are concentrated in oases that account for less than 5% of the land area [6]. Oases have long been of interest to those studying the water environment.

The desert oases in northwestern China are located along the margins of intermountain basins [7], where low precipitation and strong evaporation occur. Surface rivers are usually underdeveloped, and water for crop irrigation is recharged from rainfall in high

mountains. Since the 1970s, different hydrogeological and well completion technologies have been used to turn oases into developed, highly stable, and well-irrigated agricultural regions [8,9]. However, the uncontrolled expansion of irrigation areas, inefficient irrigation systems, and excessive groundwater exploitation has caused a series of hydroecological and environmental problems, such as groundwater funnel, groundwater pollution, soil salinization, and desert lake shrinkage. For example, the groundwater level of Minqin Oasis in Gansu Province decreases at an average rate of 0.4 to 1 m per year. In some regions, the annual fall rate of groundwater level reaches 1.12 m, and the TDS increases at a rate of 0.1–0.5 g/L per year. As a result, the shallow groundwater in this oasis no longer qualifies for irrigation [10]. Systematic research has been conducted to determine the chemical characteristics and mechanisms of groundwater recharge. Under natural conditions, groundwater quality varies from the piedmont area to the oasis and to the desert. Arid climate, groundwater burial depth, soil texture, irrigation system, and groundwater exploitation have a dramatic impact on the chemical composition of groundwater and the mechanisms of soil water and salt migration in oases [11–17]. Therefore, using long-term groundwater dynamic observation data to study the changes of hydrodynamic conditions and hydrochemical components in the process of groundwater exploitation can provide technical support for water resources management and groundwater protection, which is a compelling science research topic of groundwater resources in the desert oasis.

The Helan Mountains serve as a geographical division in China [18]. The Yinchuan Plain, lying at the eastern foot of the Helan Mountains, is an important agricultural region irrigated by water from the Yellow River. The Alxa Plateau at the western foot is a combination of desert grassland and agricultural area. In the piedmont desert region, agricultural oases are irrigated by groundwater. Some of them include Yaobao Oasis, Chahaertan Oasis, Xitan Oasis, and Chenjiajing Oasis. Growth in the immigrant population in Yaoba Oasis has encouraged the drilling of water wells. Excessive groundwater exploitation has already resulted in the instability of the ecosystem in these areas. In order to address the problems of groundwater quality deterioration and soil salinization in Yaoba Oasis, the Geological Brigade of the Hydrological Bureau of Inner Mongolia, Inner Mongolia Institute of Hydraulic Research, and Chang'an University conducted a thorough survey of the hydrogeology in Yaobao Oasis from 1980 to 2015 [19–23]. Some studies have evaluated the spatial and temporal evolution of water quality in reservoirs as well as the mechanisms of soil salinization. Since 2013, the government of Alxa League has made efforts to develop a plan for groundwater management in the oasis irrigation area. Specifically, quota management for agricultural water, water intake licensing system, tiered water pricing system, planting structure adjustment, and submembrane drip irrigation techniques have been promoted [24]. In recent years, the area reclaimed from farmland has reached 1.5×10^7 m², and the amount of exploited groundwater decreases to 33 million cubic meters per year in this region. Although the drop in water level has been limited to some degree, water quality deterioration continues. There is a need to determine the temporal and spatial distribution of groundwater quality parameters and analyze the relationship between groundwater exploitation and groundwater salinization in oases areas.

In the present research, we collected samples from the Yaoba Oasis and performed in situ and laboratory analysis to determine the chemical composition of groundwater. In addition, we used Yaoba Oasis dynamic groundwater monitoring data from 1979 to 2020 to unveil the spatial and temporal evolution of groundwater hydrochemistry in this water body for the past 40 years. For this purpose, data were analyzed using classical statistics, correlation analysis, Piper diagrams, and Gibbs diagrams [25–31]. Our ultimate goal was to determine the effect of human activities (groundwater exploitation, agricultural irrigation) on groundwater chemistry. This information may provide solutions to different problems including the increasing complexity of groundwater chemistry, groundwater quality deterioration, and heterogeneity. The research findings will shed new light on reasonable groundwater exploitation and the maintenance of healthy oasis ecosystems.

2. Materials and Method

2.1. An Overview of the Study Area

Yaoba Oasis (E 105°34'~105°39', N 38°25'~38°36') covers an area of 81 km², and it is situated along the margins of the aggraded flood plain at the western foot of Helan Mountains, with the Tengger Desert lying on the west. The oasis is a small, dustpan-shaped endorheic basin that is lower to the west and higher to the northeast [32] (Figure 1). The study area is located in the continental arid climate zone of northwestern China, where there is little rain but strong wind and evaporation. The annual precipitation decreases from north to south and from east to west. The annual precipitation in the north and south Helan Mountains is approximately 400 mm and 200–300 mm, respectively. In addition, in the west desert region, precipitation is less than 150 mm [24]. The southeast monsoon prevails in the summer. Precipitation generally occurs in the form of torrential rain from July to September every year. The annual evaporation is relatively weak in Helan Mountains range (around 1400 mm), strong in Tengger Desert (around 2000 mm).

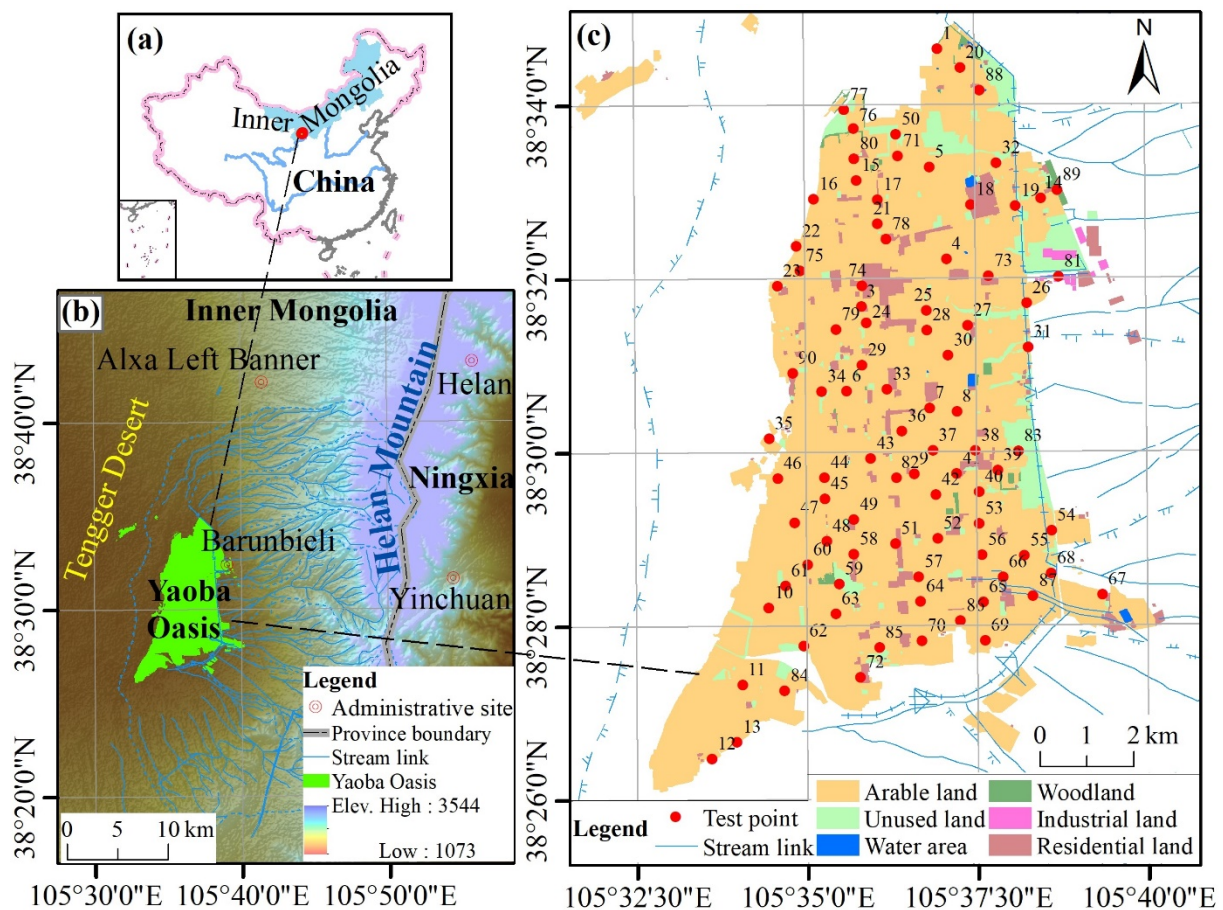


Figure 1. Map of the study region: (a) Yaoba Oasis in China; (b) Yaoba Oasis in Alxa Left Banner, Inner Mongolia Autonomous Region; and (c) land use in Yaoba Oasis and water sampling wells.

A series of north–west, north–south and east–west trending faults are located west of the Helan Mountains, resulting in a distribution pattern of structural platforms alternated with sedimentary basins [33,34]. From the piedmont region to the center of the basin, Yaoba Oasis is divided into the mountainous area, piedmont Gobi belt, oasis belt, and desert belt (or saline belt). Yaoba Oasis is located in Quaternary sedimentary basin, where the groundwater flow system presents significant variations. The aquifer beneath Yaoba consists of Quaternary sediments, dominantly fluvial, which were laid down in a faulted basin. The aquifer is underlain and bounded to the west, south and east by low permeability Tertiary and older sedimentary rocks that are effectively non-aquifers.

In Yaoba basin, Quaternary sediment is more than 200 m thick in the central part and 130 m thick in the surrounding area over the basement of Tertiary clay rock (Figure 2). The sediment in the basin has a multi-layered structure and shows two obvious sedimentary cycles from coarse to fine in the profile, which are composed of grayish yellow and brown gray sand gravel, sand, and sandy clay. Generally, there is a broad scale of Quaternary sediment grade from coarser-grained nearer to the Helan Mountains to finer-grained further from the mountains [35–37]. According to this, the Quaternary water-bearing formation is divided into two aquifer groups. The first group located at the top is 10–30 m thick, has a burial depth of 10–40 m, and contains 1–3 unstably distributed aquifers. The second group displays a more diverse lithology as medium fine sand, medium coarse sand, and pebbles are found. In this case, thickness tends to decrease from 20–40 m to 10–15 m. This layer is the primary target for groundwater exploitation for irrigation purposes. In this oasis, the groundwater body is primarily recharged by runoff from the piedmont plain area of the Helan Mountains, which flows from northeast to southwest. Later, groundwater discharges along the desert in the southwest, forming low-lying lake areas. Apart from evaporation, artificial exploitation has become the primary mechanism for the loss of pore water in the Quaternary system.

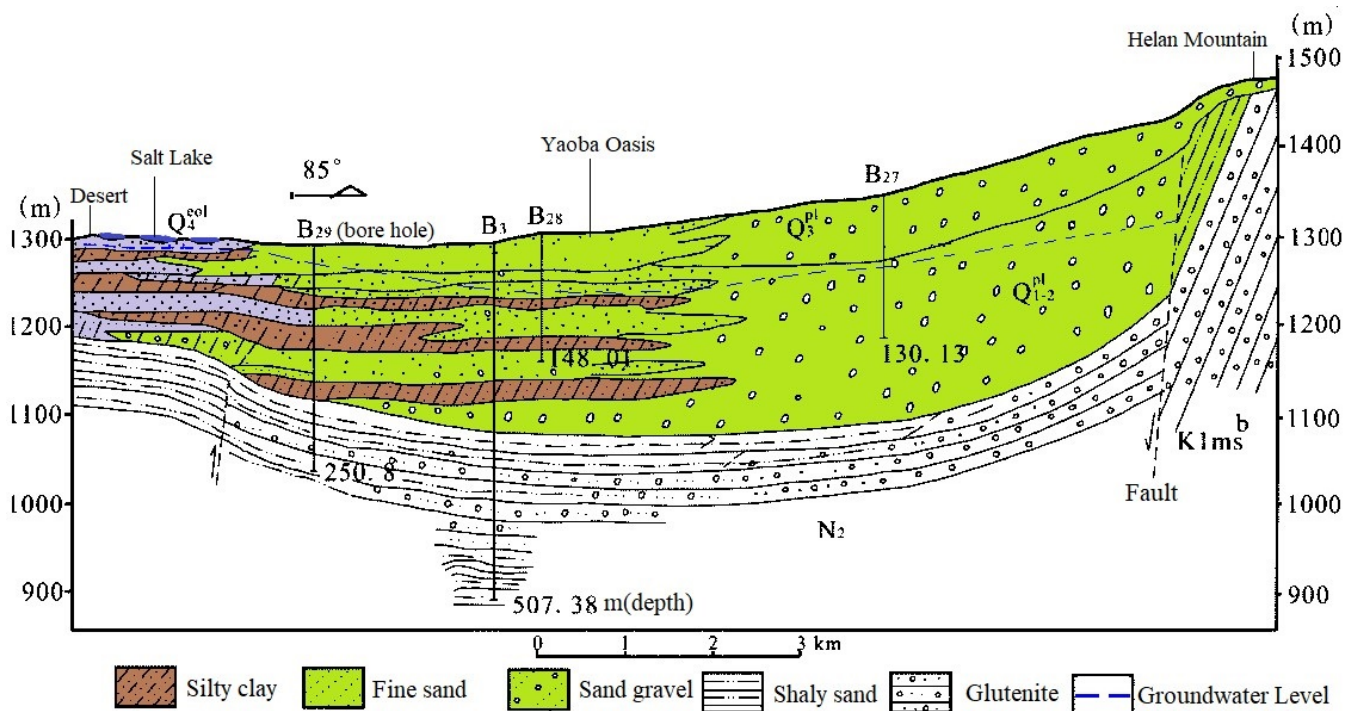


Figure 2. Hydrogeological profile of Yaoba Oasis.

2.2. Methods of Water Level Monitoring, Water Sample Collection, and Analysis

A dynamic groundwater monitoring network for well-irrigated regions in Yaoba Oasis, built in 1979, consists of 13 uniformly distributed monitoring wells that were used to monitor the groundwater of the Quaternary water-bearing formation. Continuous groundwater level records were available from six monitoring wells.

Sampling points were determined by combining remote sensing images with GPS. In order to uniformly cover the entire study area, the sampling points were spread out using a checkerboard pattern considering the distribution of motor-pumped wells. The sampling region covered an area of 81.2 km², with each sampling point representing an area of about 1.23 km². Sample collection was performed between 5 and 7 June 2020, with a total of 90 groundwater samples (Figure 1). Wells were pumped for at least 20 min to allow the borehole to be purged before sampling.

The polyethylene bottles that had been used for groundwater sampling and storage were cleaned with water and then immersed in nitric acid solution (6 mol/L) in the laboratory for about one week. After that, they were further immersed in distilled water to wash away the residual nitric acid. Finally, the bottles were cleaned with Millipore ultra-pure water and fully drained. One bucket (5 L) and two bottles (500 mL of each) were used to collect groundwater samples at each sampling point, according to the HJ 493–2009 Water Quality Sampling-technical Regulation for the preservation and handling of samples. Before sampling, the buckets and bottles were washed two to three times with the same groundwater to be sampled. For sample collection purposes, recipients were completely filled with groundwater, air was removed, and bottles were tightly sealed using paraffin wax. PH value, free carbon dioxide, conductivity and water temperature are obtained through field measurement. The accuracy of measurements for pH is ± 0.01 , for water temperature is ± 0.2 °C and for electrical conductivity is $\pm 2\%$. The weather conditions and lithology were recorded on the day of sampling. For quality control, samples were delivered to the laboratory via a cooling box within 10 days after collection and analyses were performed within 15 days.

The major components (e.g., Na^+ , K^+ , Ca^{2+} , Mg^{2+} , HCO_3^- , Cl^- , SO_4^{2-} , CO_3^{2+} , NO_3^- , pH, and total dissolved solids (TDS)) of the groundwater samples were measured at the Key Laboratory of Subsurface Hydrology and Ecological Effects in Arid Region, Chang'an University. Na^+ and K^+ were determined by flame atomic absorption spectrophotometry (GFU-202); Cl^- and SO_4^{2-} were determined by ion chromatography (HLC-601); Ca^{2+} and Mg^{2+} were determined by EDTA titration; HCO_3^- and CO_3^{2+} were determined by acid–base titration; NO_3^- was determined by potassium permanganate titration; pH was determined using the potentiometric method; and TDS was calculated by the summation of mass concentrations of all ions. The analytical precision for the measurement of major ion composition is about $\pm 5\%$ with a detection limit of 0.01 mg/L, and the ionic balance error of water samples was within $\pm 5\%$. Standards and blanks were repeatedly run to confirm the accuracy and precision of analysis.

2.3. Data Processing

Data were processed and screened using Excel. The chemical composition of groundwater samples was statistically analyzed using SPSS 24.0. The spatial distribution of the primary chemical constituents in groundwater was estimated by Kriging interpolation in Sufer, with a 1 m spatial resolution. Piper diagrams were plotted using Origin to determine the relationship between the concentrations of primary anions and cations in groundwater and assess groundwater hydrogeochemistry. Gibbs diagrams were used to identify the mechanisms controlling the formation and evolution of groundwater chemistry and analyze the origin of primary chemical constituents in groundwater.

3. Result and Analysis

3.1. Spatial Distribution of Hydrochemistry

The major dissolved components of groundwater in 90 wells were quantitatively analyzed by statistical methods. As shown in Figure 3b, groundwater pH varied between 7.38 and 7.99 with an average of 7.71, indicating a weak alkalinity. TDS varied between 581.40 and 5845.60 mg/L, with an average of 1683.81 mg/L (Figure 3a). Therefore, this area corresponds to slightly brackish groundwater ($1000 \text{ mg/L} < \text{TDS} < 3000 \text{ mg/L}$) [38]. The electrical conductivity varied between 0.74 and 5.79 ms/cm (Figure 3c), which is in agreement with the observed level of mineralization.

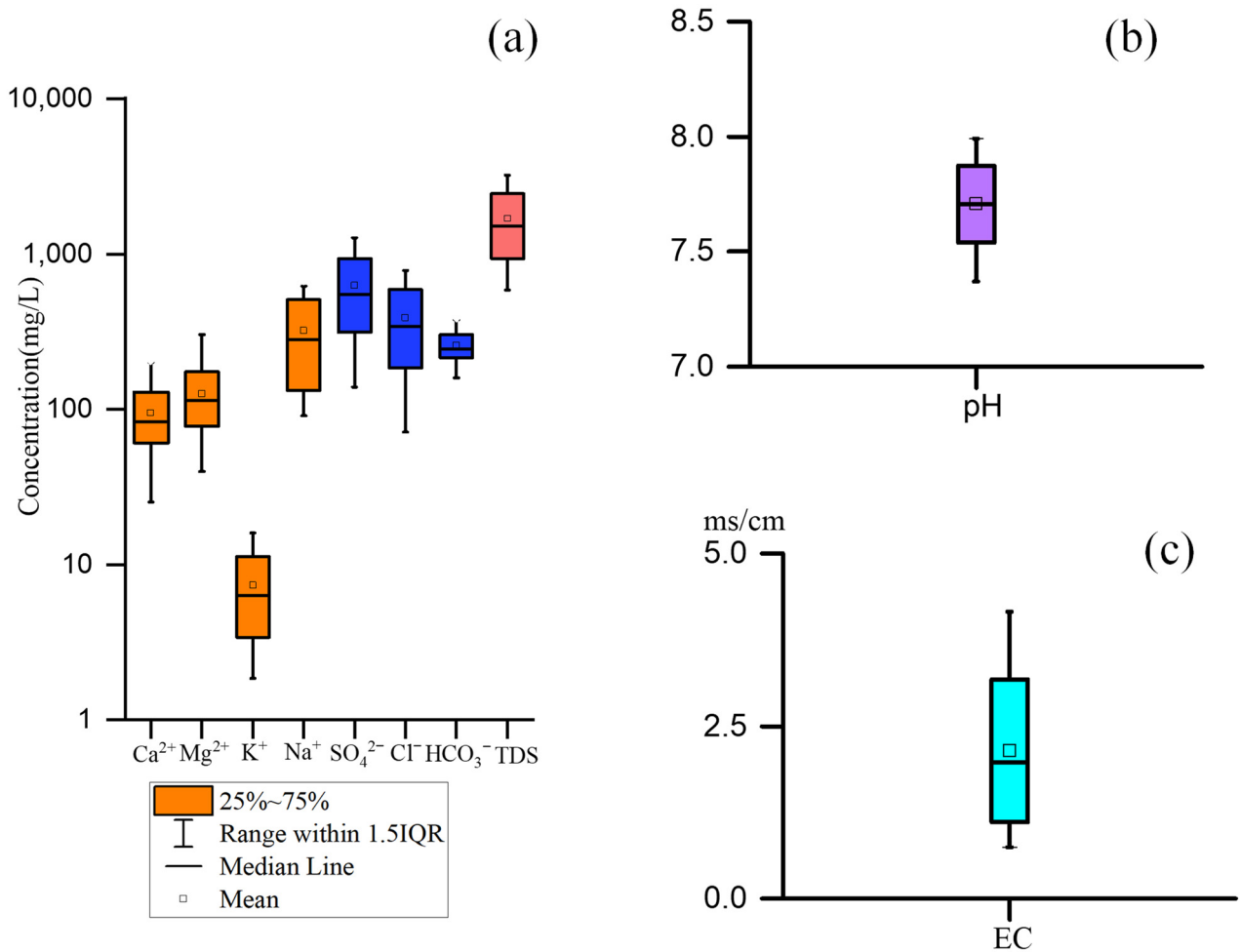


Figure 3. Boxplots of hydrochemical parameters in groundwater of the Yaoba Oasis. (a) major ions and TDS; (b) pH; (c) EC.

Isoconcentration contour maps of the main groundwater constituents were plotted using Surfer11 and differential analysis (Figure 4). Data indicated that sodium and calcium ions were the dominant cations in groundwater, while chloride and sulfate were the dominant anions. It was also observed that Ca²⁺ and HCO₃⁻ concentrations decreased along the direction of groundwater runoff (Figure 5), while Na⁺, Mg²⁺, Cl⁻ and SO₄²⁻ concentrations increased. Thus, an overall salinization trend was observed along this direction. Due to groundwater exploitation and climate factors, island-shaped zones with high Ca²⁺, Na⁺+K⁺, Cl⁻, SO₄²⁻, HCO₃⁻, and Cl⁻ concentrations were observed in Yaoba Oasis. Six areas displayed high Na⁺+K⁺ concentrations, two corresponded to high Ca²⁺ levels, five of them showed elevated SO₄²⁻ concentrations, two zones presented high HCO₃⁻ levels, and four of them showed elevated Cl⁻ accumulation. NO₃⁻ was widely present in groundwater used for agricultural irrigation. In some wells, F⁻ and Mn²⁺ concentrations exceeded the limits for drinking water [29]. F-rich groundwaters are well explained by the dissolution of granite containing fluorite, and the progressive dissolution of fluorite is possible due to the decreasing calcium concentration [39]. This result indicated the increasing complexity of groundwater chemistry along with groundwater quality deterioration and heterogeneity. The hydrochemical action was intensifying.

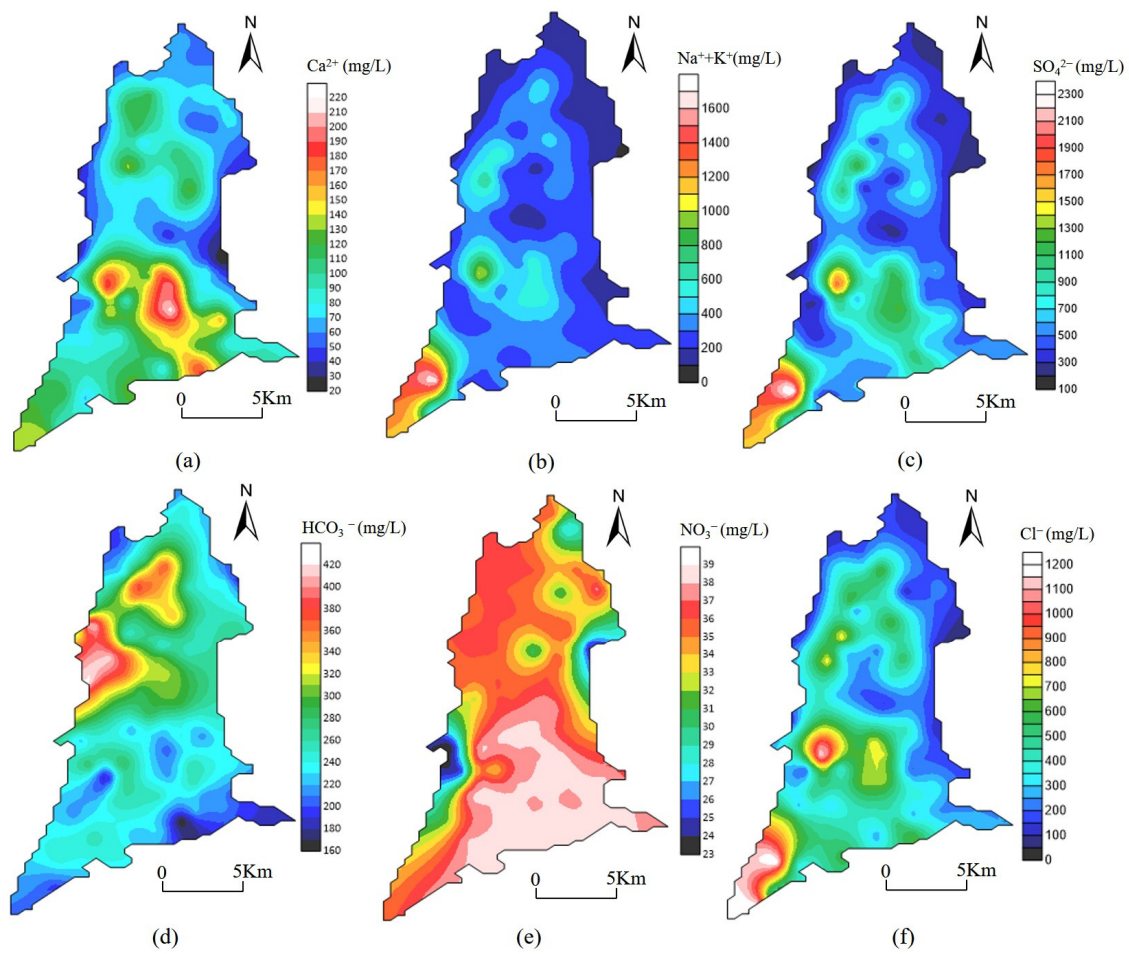


Figure 4. Spatial distribution of main ions in groundwater of Yaoba Oasis. (a) Ca^{2+} ; (b) $\text{Na}^{+}+\text{K}^{+}$; (c) SO_4^{2-} ; (d) HCO_3^{-} ; (e) NO_3^{-} ; (f) Cl^{-} .

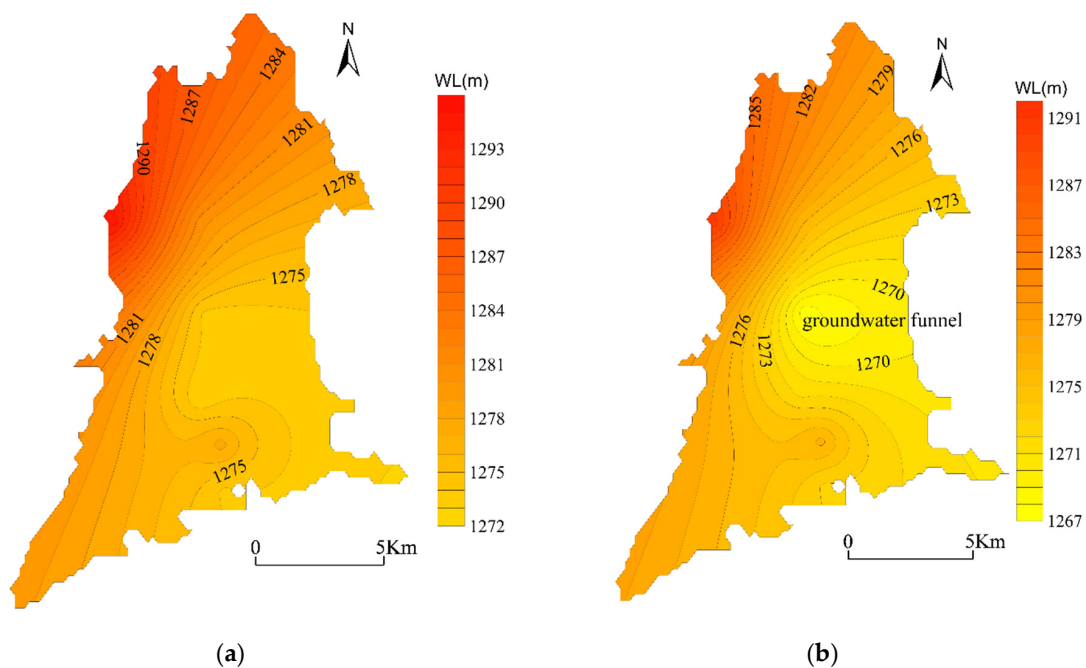


Figure 5. Groundwater Level Contour Maps for Yaoba Oasis during non-irrigation season (January) and irrigation season (July). (a) January 2020; (b) July 2020.

There are a large number of wells in the south of Yaoba Oasis that have elevated nitrate with increased salinity, chloride, and sulfate (Figure 2). All these wells were within the irrigated cropland and may indicate apparent degradation of the groundwater from excess fertilizer and manure leached by irrigation return flow. Such irrigation return flow carries high concentrations of NO_3^- and dissolves large amounts of soluble salts as it filters down through the vadose zone. At first, salts enter the shallow groundwater, increasing the degree of groundwater mineralization. When these species travel to deeper areas, they pollute groundwater, resulting in local regions of elevated groundwater mineralization. Intensive and extensive use of pesticides and fertilizers over the years is another reason for the increasing TDS and NO_3^- in groundwater.

In the study area, TDS increased from 581.4 to 5845.80 mg/L along the direction of groundwater runoff. In addition, three high values of TDS were observed as shown in Figure 6a: (a) a slightly brackish water area with TDS of 2200–3000 mg/L in the north of the oasis; (b) a slightly brackish water area with TDS of 2000–3000 mg/L in the middle of the oasis, where some samples reached TDS values up to 4000 mg/L indicating the presence of salty water; and (c) a salty lake in the desert located in the southwest part of the oasis, where groundwater displayed the highest TDS values above 3000 mg/L. Apart from the high TDS zones, areas with low levels of TDS were found. This indicated the presence of freshwater. TDS in some wells along the margins of northwest–north–northeast–east and in the middle of the oasis was below 1000 g/L.

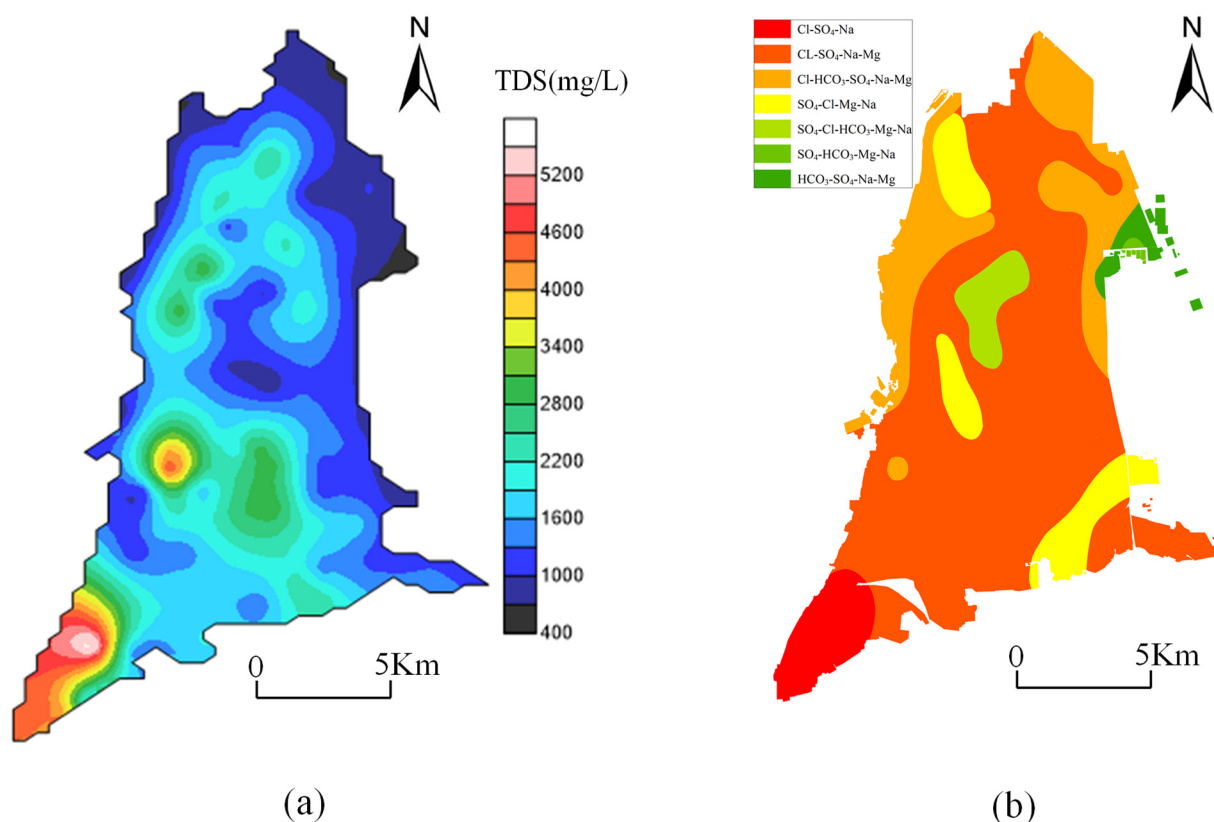


Figure 6. Spatial Distribution of TDS and hydrochemical water type. (a) TDS; (b) hydrochemical type.

3.2. Spatial Evolution Law of Groundwater Hydrochemistry

The hydrochemical types map (Figure 6b) and Piper diagrams (Figure 7a) were plotted for 90 wells of groundwater samples. Data indicated that hydrochemical types of groundwater in the study area were highly diversified. The dominant types were Cl·SO₄-Na·Mg, Cl·HCO₃-SO₄-Na·Mg, SO₄-Cl-Mg·Na, SO₄-Cl·HCO₃-Mg·Na, and Cl·SO₄-Na. In addition, it was observed that the hydrochemical type presented a complex pattern from northeast to southwest along the direction of groundwater runoff. A transition was observed from

$\text{HCO}_3\text{-SO}_4\text{-Na}\cdot\text{Mg}$ and $\text{Cl}\cdot\text{HCO}_3\text{-SO}_4\text{-Na}\cdot\text{Mg}$ to $\text{Cl}\cdot\text{SO}_4\text{-Na}\cdot\text{Mg}$ and then to $\text{Cl}\cdot\text{SO}_4\text{-Na}$. In the middle of the oasis, SO_4^{2-} and Mg^{2+} concentrations increased sporadically, resulting in an island-shaped distribution of $\text{SO}_4\text{-Cl}\cdot\text{Mg}\cdot\text{Na}$ and $\text{SO}_4\text{-Cl}\cdot\text{HCO}_3\text{-Mg}\cdot\text{Na}$. As shown in the Piper diagrams (Figure 7a), groundwater samples were distributed in a more diffuse manner to the west than to the east and in the middle of the oasis. Instead of a simple transition toward the $\text{Cl}\cdot\text{SO}_4\text{-Na}$ type, HCO_3^- concentration increased from the northern area to the northwest, where the $\text{Cl}\cdot\text{HCO}_3\text{-SO}_4\text{-Na}\cdot\text{Mg}$ type appeared. In addition, the $\text{SO}_4\text{-Cl}\cdot\text{Mg}\cdot\text{Na}$ water was identified to the north of where the $\text{Cl}\cdot\text{HCO}_3\text{-SO}_4\text{-Na}\cdot\text{Mg}$ type was detected. Indeed, the Total Ionic Salinity (TIS) of waters ranges from 991.7 to 7869.4 mg/L (Figure 7b). The samples of ground waters fall into four groups (0~2000 mg/L, 2000~4000 mg/L, 4000~6000 mg/L and 6000 mg/L~8000 mg/L). Most data are located between 2000 and 4000 mg/L.

Yaoba Oasis is a hydrogeological unit on the margins of the typical aggraded flood plain. Here, the groundwater mainly comes from the underground water area belonging to the Quaternary water-bearing formation. In well-irrigated areas, water is mainly exploited from aquifers composed of gravel-bearing medium fine sand, medium coarse sand, fine sand, and coarse sand. Groundwater runoff generally flows from northeast to southwest. In the recharge zones located in the northeast oasis area, the runoff alternates rapidly, carrying salts along with it. As dolomite and calcite were dissolved, Mg^{2+} and Ca^{2+} became the main groundwater constituents. These ions and TDS were significantly correlated. The dominant hydrochemical types corresponded to $\text{SO}_4\text{-Cl}\cdot\text{Ca}\cdot\text{Mg}$ and $\text{SO}_4\text{-HCO}_3\text{-Cl}\cdot\text{Mg}\cdot\text{Na}$. As runoff slowed down in the middle of the oasis, the hydrochemical type $\text{Cl}\cdot\text{SO}_4\text{-Ca}\cdot\text{Mg}$ appeared. In the discharge area in the southwest oasis zone, low groundwater flow rates and elevated evaporation and concentrations were observed. Therefore, water was depleted and salts remained. Thus, $\text{Na}^+\text{+K}^+$, SO_4^{2-} , and Cl^- became the main ions in groundwater, which were significantly correlated with TDS. Here, the dominant water was the $\text{SO}_4\text{-Cl}\cdot\text{Ca}\cdot\text{Na}$ type.

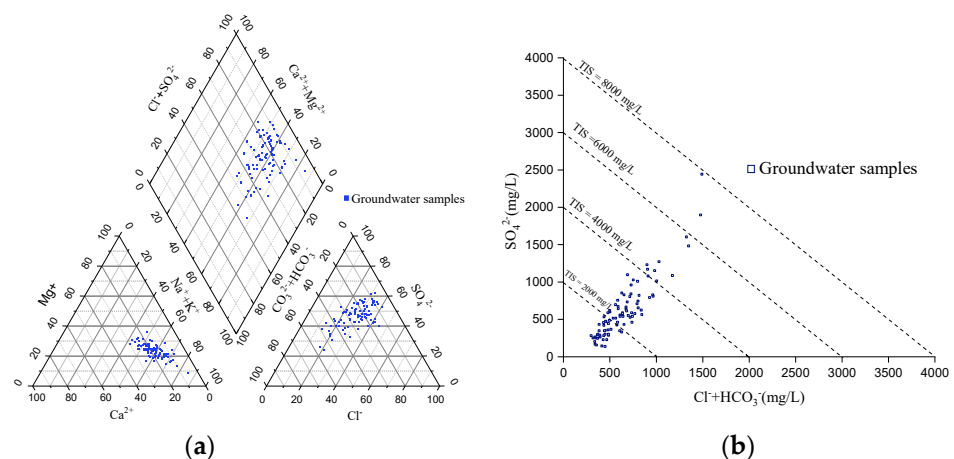


Figure 7. All 90 wells of groundwater samples shown in (a) Piper diagram and (b) Total Ionic Salinity (TIS) diagram.

3.3. Hydrochemical Formation Mechanism of Groundwater

We performed Pearson correlation analysis [36,40] to determine the strength of correlation among different chemical constituents present in the groundwater of the oasis (Table 1). The correlation matrix indicates that correlation coefficient of major ions is positive except HCO_3^- and TDS. TDS has a quite positive and closely correlation with SO_4^{2-} , Cl^- , $\text{K}^+\text{+Na}^+$, Mg^{2+} , and Ca^{2+} , whose correlation coefficients of chemical components are more than 0.5. Moreover, the correlation coefficients between SO_4^{2-} and $\text{K}^+\text{+Na}^+$, SO_4^{2-} and Cl^- is great than 0.95; there appeared to be a strong correlation. Under a high level of mineralization, SO_4^{2-} , Cl^- , and Na^+ contents increased significantly. In the piedmont recharge area of the Helan Mountains, dolomite and calcite are dissolved. As a result, Mg^{2+}

and Ca^{2+} are the main ions in groundwater, which were significantly correlated with TDS. In addition, groundwater runoff is able to dissolve dolomite and calcite, gypsum, halite, potassium salts, and fluorite. Due to calcium ion adsorption and sodium ion desorption, $\text{Na}^+ + \text{K}^+$, SO_4^{2-} and Cl^- were the main ions in groundwater, which were significantly correlated with TDS.

Table 1. Correlation coefficients between different chemical parameters in the study area.

Item	Ca^{2+}	Mg^{2+}	$\text{K}^+ + \text{Na}^+$	SO_4^{2-}	Cl^-	HCO_3^-	NO_3^-	TDS	CO_2	pH	Electrical Conductivity
Ca^{2+}	1										
Mg^{2+}	0.811 **	1									
$\text{K}^+ + \text{Na}^+$	0.551 **	0.667 **	1								
SO_4^{2-}	0.770 **	0.833 **	0.932 **	1							
Cl^-	0.763 **	0.876 **	0.907 **	0.932 **	1						
HCO_3^-	-0.310 **	0.059	0.041	-0.07	-0.043	1					
NO_3^-	0.475 **	0.398 **	0.296 **	0.423 **	0.348 **	-0.124	1				
TDS	0.751 **	0.852 **	0.952 **	0.987 **	0.974 **	-0.011	0.387 **	1			
CO_2	0.301 **	0.398 **	0.154	0.273 **	0.245 *	0.136	0.113	0.261 *	1		
pH	-0.426 **	-0.386 **	-0.09	-0.262 *	-0.227 *	0.088	-0.194	-0.234 *	-0.636 **	1	
Electrical conductivity	0.857 **	0.959 **	0.916 **	0.960 **	0.978 **	0.017	0.414 **	0.985 **	0.343 **	-0.357 **	1

Note: ** Significantly correlated at the 0.01 level (two-sided); * Significantly correlated at the 0.05 level (two-sided).

The Gibbs diagrams can be used to represent the relationship between TDS vs. $\text{Na}/(\text{Na} + \text{Ca})$ and $\text{Cl}/(\text{Cl} + \text{HCO}_3)$ in rivers, lakes and oceans. The three mechanisms controlling the chemical components in natural waters include atmospheric precipitation, rock weathering, and evaporation. Recently, Gibbs diagrams have been extensively applied to represent the controlling mechanisms of hydrochemistry in groundwater [40–44].

We plotted TDS vs. $\text{Na}/(\text{Na} + \text{Ca})$ and TDS vs. $\text{Cl}/(\text{Cl} + \text{HCO}_3)$ using the groundwater sample data of the Yaoba Oasis, as shown in Figure 8.

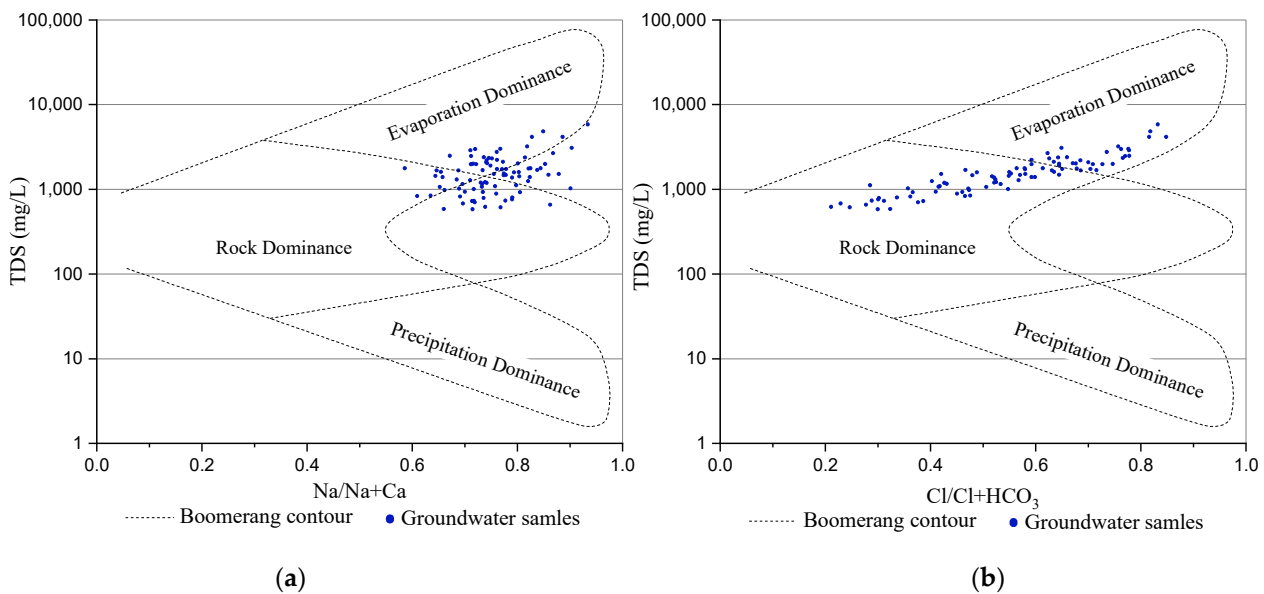


Figure 8. Gibbs diagram showing the mechanisms controlling groundwater chemistry in the study area. (a) major cations vs. TDS; (b) major anions vs. TDS.

High TDS levels were found in groundwater of the Yaobao Oasis. The $\text{Na}/(\text{Na} + \text{Ca})$ and $\text{Cl}/(\text{Cl} + \text{HCO}_3)$ ratios varied within 0.6–1 and 0.2–0.8, respectively. Most groundwater samples were distributed in the middle to the upper parts of the Gibbs diagrams. According to our results, evaporation was the dominant mechanism controlling groundwater chemistry. Notably, around 80% of groundwater samples represented evaporation dominance, evaporation made salinity accumulate by increasing Na^+ and Cl^- with relation to high

concentration of TDS, and $\text{Cl}/(\text{Cl}+\text{HCO}_3)$ ratio rose correspondingly above 0.6 (Figure 8). Since Yaoba Oasis sits on the eastern margin of the Tengger Desert, therefore, it reveals meteorological characteristics of arid climate with high evaporation and low rainfall. The Gibbs diagrams showed that as TDS increased, the $\text{Na}/(\text{Na}+\text{Ca})$ and $\text{Cl}/(\text{Cl}+\text{HCO}_3)$ ratios also increased. The groundwater samples were densely distributed in the upper part of the Gibbs diagrams. Thus, the groundwater chemistry in Yaoba Oasis was mainly controlled by evaporation. Moreover, the groundwater discharge area (salty lake in the southwest part of the oasis) significantly affected the chemical characteristics of groundwater in this area.

Binary diagrams, saturation indices and any geochemical equilibrium models are important tools to reconstruct the groundwater–rock interaction process in these various environments [45–47]. It should be noted that the saturation indices (SI) of minerals are useful for evaluating the extent to which water chemistry is controlled by equilibrium with solid phases [48,49], and according to the geological and mineral research data of the study area, the main dissolved minerals constituting the water-bearing sedimentary rocks are mainly calcite, dolomite, rock salt and gypsum. The PHREEQC geochemical model was used to calculate the saturation index (SI) for common minerals and the distribution of major ions. The calculation results show that calcite and dolomite is over-saturation ($\text{SI} > 0$), whereas rock salt and gypsum are undersaturated (Figure 9). Along the groundwater runoff direction, the behaviors of water–rock interaction are manifested by the precipitation of calcite and dolomite and the dissolution of rock salt and gypsum with TDS increasing.

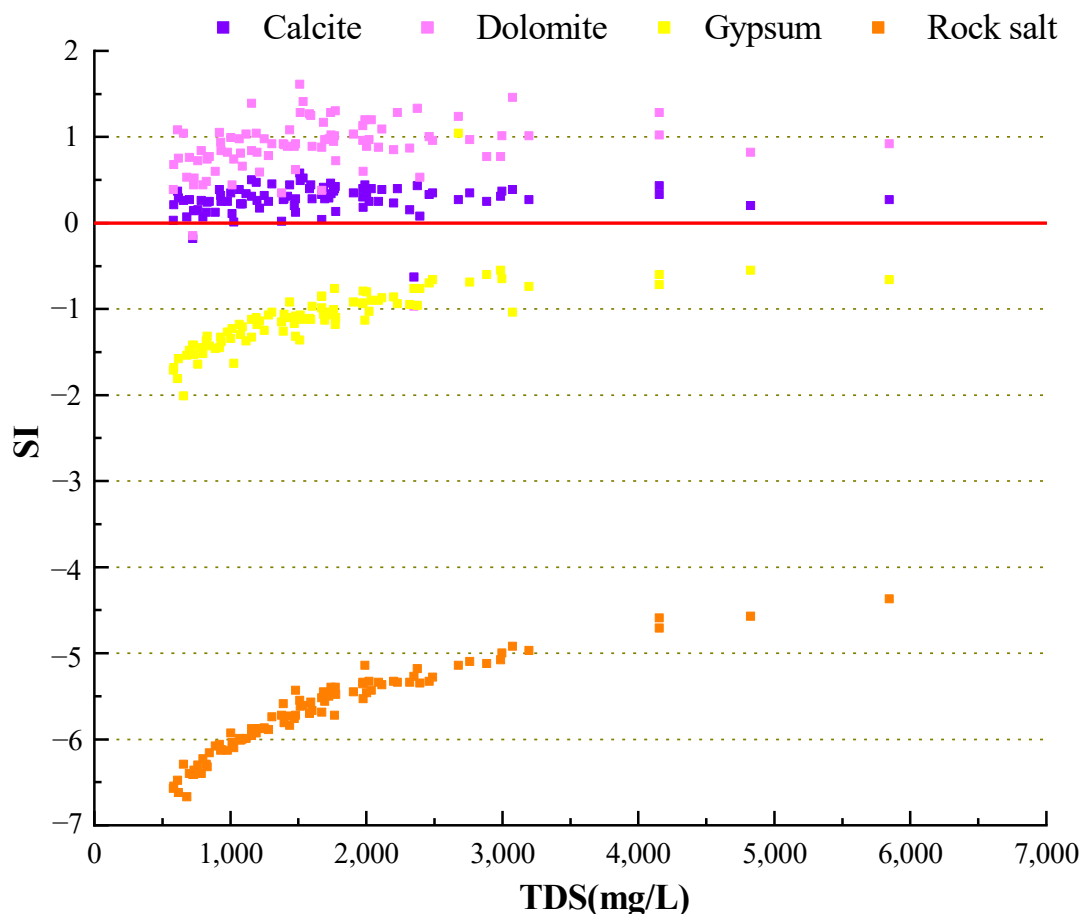


Figure 9. Relationship between saturation indices of main minerals and TDS in the study area.

4. Discussion

The groundwater quality and chemical process is affected by several factors in the oasis–desert region, such as geological conditions, runoff, land use types, groundwater exploitation, and agricultural activities [43,50–52]. The chemical composition of ground-

water in Yaoba Oasis was closely related to residual salts in the Quaternary sedimentary environment. Since the late Pleistocene, a series of fan-fringing depressions that have been formed under arid climate in Yaoba Oasis contain fine-grained deposits with high salinity and lenticular distribution [53]. They provide a source of substances that increases the degree of mineralization in shallow groundwater. Beyond that, the aforementioned particular analysis of the chemistry data suggests that flood irrigation returns are seriously degrading the quality of the groundwater in the aquifer. The infiltration of irrigation water will increase the risk of groundwater contamination by nitrogen pollution and salinization [54]. As a result, salt levels in soil increase with depth after 50 cm below surface. These salts also contribute to groundwater salinization. In the vadose zone, a large amount of irrigation water returns and infiltrates in areas with high permeability where no aquifers are present. The infiltrating groundwater dissolves the salts in the rock, further entering the aquifer. Because of this process, salt levels abruptly increase.

Groundwater chemical evolution is a long-term, complex process involving water–rock interactions [55–57]. The groundwater chemical field in the oasis can reflect the groundwater dynamic conditions to a certain degree. In the past 40 years, groundwater exploitation in Yaobao Oasis can be divided into three stages (Figure 6): (a) from 1980 to 1989, the amount of groundwater exploitation was maintained between 22.611 and 25.295 million cubic meters per year. In addition, because of climate factors, the level of groundwater at the three monitoring wells changed 0.3 m per year. In this area, TDS showed concentrations below 550.92 mg/L. From 1990 to 2013, the well-irrigated regions in the oasis expanded to $6.13 \times 10^7 \text{ m}^2$, and the amount of groundwater exploitation increased to 47.5781 million cubic meters per year. The groundwater level declined at an annual average rate reach of 1.13 m/a (No. 13 well). In the middle and southwestern parts of the oasis, a highly mineralized region of 20.8 km² was formed. In the monitoring well, groundwater TDS increased from 1292.56 to 2267.74 mg/L. From 2013 to 2020, the government implemented a series of water conservation measures. After that, the groundwater level in the well-irrigated regions decreased at a lower rate (0.213–1.09 m in total). The annual average drop rate of groundwater level was 0.036–0.181 m. Some locations reported a small rise in groundwater level (No. 11 well). Nevertheless, groundwater TDS in the monitoring well continued to increase slowly, with an annual increase rate of 49.36 mg/L. Thus, groundwater quality deterioration continued. The reason was that in the desert lake, the level of groundwater was higher than that in the funnel area of the oasis. Moreover, the dynamic conditions for the transport of highly mineralized salty water to the desert in the southwestern part of the oasis remained the same.

Human factors that influence hydrochemical processes are mainly related to the types and intensities of human activities [58]. Excessive groundwater exploitation has resulted in the continuous drop of groundwater level in the oasis [59]. As shown in the well data from 1989 to 2020, the groundwater level dropped at a rate of 0.22–0.3 m/a. The total reduction in groundwater level in these years was 4.5–6.8 m (Figure 10). A descending funnel is observed in the middle of the oasis. At the center of the funnel, the groundwater level decreased to 1272.3–1278.1 m, which is smaller than that of the desert salty lake by 2.34 m. In the discharge area in the western part of the oasis, groundwater returns to the zone where the present investigation was performed (Figure 11a). In the meantime, the considerable hydraulic gradient in the descending funnel increases the probability of overflow into the aquifer, which further enhances the mixing and leaching effects of different types of water near the descending funnel. As the direction of groundwater runoff changes, the salty water in the southwestern part of the oasis enters the study area. Therefore, those regions with high TDS concentrations continue to increase. Because of this, the area where groundwater salinization occurs also expands. This situation is exacerbated by the infiltration of irrigation return flow under flooding irrigation and the leaching of residual salts in the vadose zone (Figure 11b). For this reason, groundwater hydrochemistry diversifies. In conclusion, groundwater exploitation has altered the groundwater flow field and also the modes of water circulation and water–salt migration in the oasis. As a result,

intensified water–rock interactions have become the most important driving forces behind the groundwater chemical evolution in the desert oasis.

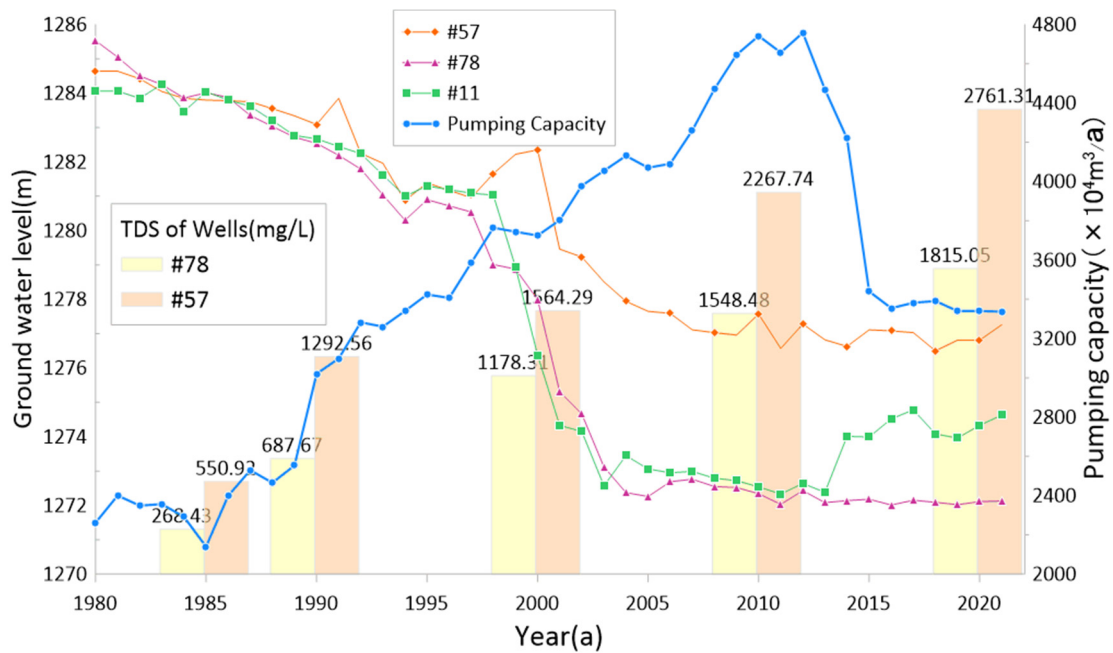


Figure 10. Relationship between pumping capacity, water level, and TDS in groundwater of the Yaoba Oasis.

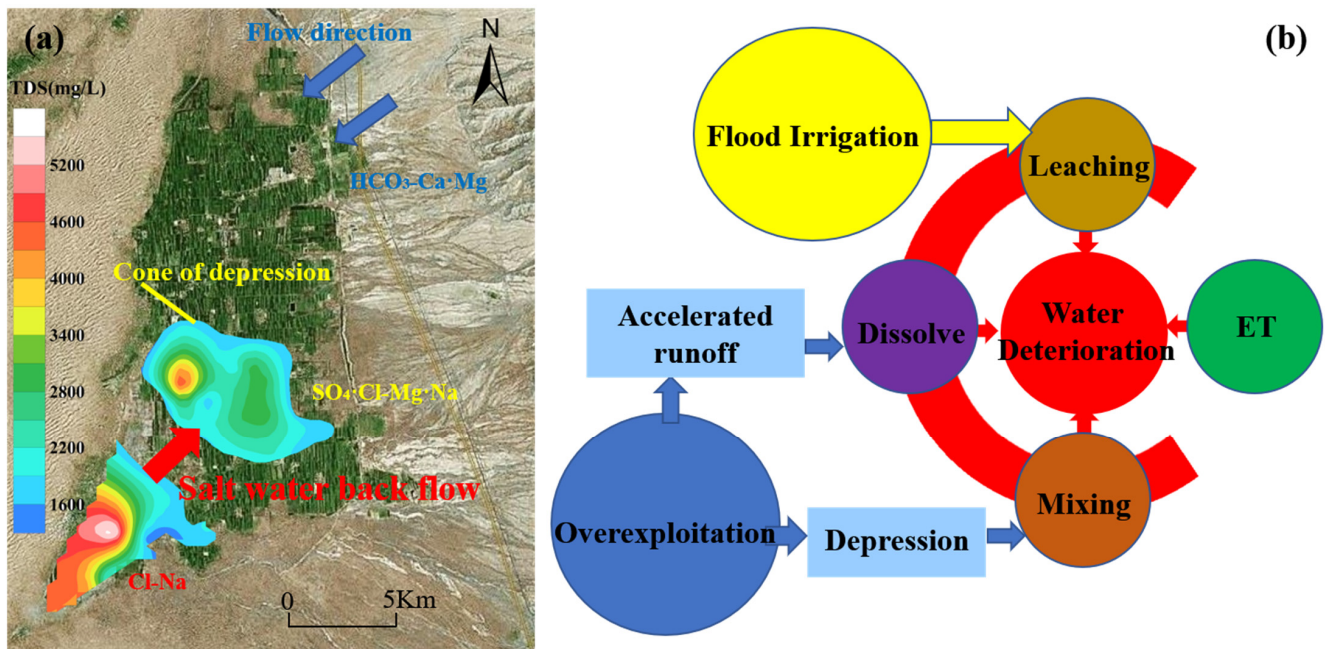


Figure 11. Process of salinization in groundwater of the Yaoba Oasis. (a) Groundwater degradation under salt water intrusion; (b) Groundwater hydrochemical response to overexploitation.

To prevent further groundwater deterioration and maintain the oasis–irrigation ecosystems in the arid areas, it is urgent to provide some feasible solutions for optimizing groundwater resources allocation and improving groundwater environment [59]. Since 2013, the government of Alxa League has made significant efforts to improve groundwater management in the oasis irrigation area. Specifically, quota management for agricultural water,

water intake licensing system, tiered water pricing system, planting structure adjustment, and submembrane drip irrigation have been reinforced [60,61]. In recent years, the area reclaimed from farmland has reached 1.5×10^7 m², and the amount of exploited groundwater has decreased to 33 million cubic meters per year in this region. Although the drop in water level has been limited to some degree, the groundwater quality deterioration persists. Our results indicate that the groundwater dynamic conditions for salty water intrusion have not significantly changed. To protect and remediate the groundwater environment in the oasis and allow the natural recharge process, the amount of groundwater exploitation in the area should be restricted to 22 million cubic meters per year and groundwater level maintained above that corresponding to the desert lake (1275 m). These two actions will recover the balance between groundwater exploitation and recharge.

5. Conclusions

This study has revealed the temporal and spatial distribution of groundwater chemical components, and its hydrogeologic and hydrochemical processes in Yaoba Oasis, China. The conclusion is as follows:

- (1) Water salinity in Yaoba Oasis increased in the direction of groundwater runoff. In addition, Ca²⁺ and HCO₃⁻ concentrations in groundwater decreased, while those of Na⁺, Mg²⁺, Cl⁻, and SO₄²⁻ increased over time. Moreover, the levels of TDS in groundwater augmented, and according to hydrochemical data, the type of water changed from HCO₃·SO₄-Na·Mg to Cl·SO₄-Mg·Na and later to Cl·SO₄-Na.
- (2) Because of groundwater exploitation and climate factors, the hydrochemical types displayed island-shaped distribution patterns from the northeast to the southwest. As the hydrochemical type changed, complexity increased. Island-shaped distribution of SO₄-Cl-Mg·Na and SO₄-Cl-HCO₃-Mg·Na type water was observed near the descending funnel in the oasis. As a result of evaporation, the Cl·SO₄-Na type water was formed in the discharge area of the desert salty lake in the southwest part of the oasis.
- (3) Groundwater quality deterioration in the oasis results from the joint action of the infiltration of irrigation return flow and the intrusion of salty water in the desert lake area. The former only makes a limited contribution to groundwater salinization, while the latter is the main reason for groundwater salinization in the irrigated areas. The high value area of soluble salt ions (Na⁺, Mg²⁺, Cl⁻, SO₄²⁻) and the island area with abnormal groundwater hydrochemical type in the study area are basically consistent with the groundwater depression funnel area of the oasis.

Herein, we report the groundwater chemical characteristics and evolution process in Yaobao Oasis. On this basis, we proposed an optimization scheme for the reasonable development and exploitation of groundwater resources, which primarily consider the replacement of flooding irrigation with water-saving irrigation techniques. Our findings provide scientific insights for sustainable agricultural development in the desert oases of Northwestern China.

Author Contributions: Conceptualization, A.H. and T.L.; methodology, A.H. and T.L.; investigation, T.L., J.W., Y.L. and W.Z.; resources, A.H. and W.Z.; data curation, J.W. and Y.L.; writing—original draft preparation, A.H. and T.L.; writing—review and editing, J.W. and Y.L.; project administration, W.Z.; funding acquisition, A.H. All authors have read and agreed to the published version of the manuscript.

Funding: This work was supported by the National Natural Science Foundation of China (Grant No. 41877232, 41790444, 41672255 and U2243204).

Data Availability Statement: Not applicable.

Acknowledgments: The authors thanked the two anonymous reviewers and the editor for their constructive comments, which significantly improved the quality of this article.

Conflicts of Interest: The authors declare that there is no conflict of interest regarding the publication of this paper.

References

- Zhang, F.; Lai, X.; Pan, X. Characteristics of Desert Improving Temperature Effect and Distribution of Oasis Agricultural Heat Resource. *J. Desert Res.* **2004**, *24*, 751–754.
- Luo, G.; Zhou, C.; Chen, X.; Zhou, K. Evaluation of the stability of the oasis at the regional scale. *J. Nat. Resour.* **2004**, *19*, 519–524.
- Hu, R.; Fan, Z.; Wang, Y.; Jiang, F. Groundwater resources and their characteristics in arid lands of Northwestern China. *J. Nat. Resour.* **2002**, *17*, 321–326.
- Ma, X.-W.; Lu, Y.-Z.; Li, B.-G.; Zhu, J.-R. A Model to Simulate Temporal-spatial Change of Groundwater Mineralization Resulted from Land Use in Oasis. *J. Nat. Resour.* **2009**, *24*, 268–275.
- Hu, Y.; Zhang, Y.; Han, Y. Identification and monitoring of desertification lands in China from 2000 to 2015. *Arid Land Geogr.* **2018**, *41*, 1321–1332.
- Li, W. Theory and Practice of Oasis Ecological Economic Sustainable Development. *Chin. Rural Econ.* **2003**, *18*, 47–51.
- Chen, M. Rational Development and Utilization of Water Resources Related to Prevention of Desertification in Arid Area of North-west China. *J. Earth Sci. Environ.* **2005**, *27*, 1–7.
- Huo, A.D.; Yang, L.; Luo, P.P.; Cheng, Y.X.; Peng, J.B.; Nover, D. Influence of landfill and land use scenario on runoff, evapotranspiration, and sediment yield over the Chinese Loess Plateau. *Ecol. Indic.* **2021**, *121*, 107208. [[CrossRef](#)]
- Cheng, Y.X.; Huo, A.D.; Zhao, Z.X.; Peng, J.B. Analysis of loess fracture on slope stability based on centrifugal model tests. *Bull. Eng. Geol. Environ.* **2021**, *80*, 3647–3657. [[CrossRef](#)]
- Cao, L.; Nie, Z.; Liu, M.; Lu, H.; Wang, L. Changes in natural vegetation growth and groundwater depth and their relationship in the Minqin oasis in the Shiyang River Basin. *Hydrogeol. Eng. Geol.* **2020**, *47*, 25–33.
- Zhang, J.; Huo, A.D.; Zhao, Z.X.; Yang, L.Y.; Peng, J.B.; Cheng, Y.X.; Wang, Z.F. Impact of Mountain Reservoir Construction on Groundwater Level in Downstream Loess Areas in Guanzhong Basin, China. *Water* **2022**, *14*, 1470. [[CrossRef](#)]
- Wei, S.; Guo, Y.; Cui, Y.; Zhang, Q.; Shao, J. Dynamic characteristics of groundwater level and storage variables in Minqin from 1985 to 2016. *Arid Land Geogr.* **2021**, *44*, 1272–1280.
- Wang, X.; Shao, J.; Wang, Z.; Cui, Y.; Zhang, Q. A study of the determination of indicators of dual control of groundwater abstraction amount and water table in northwest China: A case study of the Minqin Basin. *Hydrogeol. Eng. Geol.* **2020**, *47*, 17–24.
- Ma, J.Z.; Wang, X.S.; Edmunds, W.M. The characteristics of groundwater resources and their changes under the impacts of human activity in the arid northwest China—A case study of the Shiyang River Basin. *J. Arid Environ.* **2005**, *61*, 277–295. [[CrossRef](#)]
- Li, H.; Feng, Q.; Chen, L.; Zhao, Y.; Yang, H. Hydrochemical Characteristics and Evolution Mechanism of Groundwater in the Minqin Oasis. *Arid Zone Res.* **2017**, *34*, 733–740.
- Huo, A.; Zhao, Z.; Luo, P.; Zheng, C.; Peng, J.; Abuarab, M.E.-S. Assessment of Spatial Heterogeneity of Soil Moisture in the Critical Zone of Gully Consolidation and Highland Protection. *Water* **2022**, *14*, 3674. [[CrossRef](#)]
- Huo, A.; Wang, X.; Zhao, Z.; Yang, L.; Zhong, F.; Zheng, C.; Gao, N. Risk Assessment of Heavy Metal Pollution in Farmland Soils at the Northern Foot of the Qinling Mountains, China. *Int. J. Environ. Res. Public Health.* **2022**, *19*, 14962. [[CrossRef](#)] [[PubMed](#)]
- Han, D. The progress of research on oasis in China. *Sci. Geogr. Sin.* **1999**, *19*, 313–319.
- Zheng, C.; Lu, Y.; Guo, J.; Li, H. Soil Water Infiltration Characteristics in Oasis on West Side of Helan Mountains. *Bull. Soil Water Conserv.* **2017**, *37*, 146.
- Wang, Q.-H.; Lu, Y.-D.; Sai, J.-M.; Li, H.-H. Characteristics of Soil Salinity in Arid Oasis. *Arid Zone Res.* **2018**, *35*, 503–509.
- Sai, J.; Lu, Y.; Wang, Z.; He, M. Characteristics of Soil Salinization in Yaoba Oasis of Inner Mongolia Autonomous Region. *Bull. Soil Water Conserv.* **2017**, *37*, 152–156.
- Ling, J.; Peicheng, L.I.; Anyan, H.U.; Zhonghua, X.U. The groundwater chemical characteristics in the Yaoba oasis of Alxa area, Inner Mongolia. *J. Arid Land Resour. Environ.* **2009**, *23*, 105–110.
- Li, X.; Lu, Y.D.; Zhang, X.Z.; Zhang, R.; Fan, W.; Pan, W.S. Influencing Factors of the Spatial-Temporal Variation of Layered Soils and Sediments Moistures and Infiltration Characteristics under Irrigation in a Desert Oasis by Deterministic Spatial Interpolation Methods. *Water* **2019**, *11*, 1483. [[CrossRef](#)]
- Wang, Q.; Lu, Y. Hydrochemical characteristics and causes of groundwater in Yaoba Oasis of Inner Mongolia. *J. Huazhong Agric. Univ.* **2021**, *40*, 81–88.
- Zhao, J.; Zhou, J.; Liang, C.; Yin, Z.; Bao, Z.; Qian, L. Hydrogeochemical process of evolution of groundwater in plain area of Yanqi, Xinjiang. *Environ. Chem.* **2017**, *36*, 1397–1406.
- Zhang, Y.; Wu, Y.; Yang, J.; Sun, H. Hydrochemical Characteristic and Reasoning Analysis in Siyi Town, Langzhong City. *Environ. Sci.* **2015**, *36*, 3230–3237.
- Wang, X.; Xu, X.; Chai, C.; Zhang, Y. Spatial Distribution of Brackish Groundwater and Its Formation Causes in the Minqin Oasis in Lower Reaches of the Shiyang River. *Arid Zone Res.* **2014**, *31*, 193–200.
- Shanyengana, E.S.; Seely, M.K.; Sanderson, R.D. Major-ion chemistry and ground-water salinization in ephemeral floodplains in some arid regions of Namibia. *J. Arid Environ.* **2004**, *57*, 211–223. [[CrossRef](#)]
- Peng, L.; Bi Lali-Yi, M.; Wan, Y.; Guo, Y.; Shi, Q. Hydrochemical characteristics of shallow groundwater in Dali yaboyi oasis in the hinterland of the desert. *J. Arid Land Resour. Environ.* **2021**, *35*, 88–95.
- Niu, Y.; Liu, J.; Zhang, H.; Bian, B.; Zhao, G. Correlation analysis among precipitation and soil water and groundwater in oasis-desert transitional belt in Heihe river middle reaches. *J. Cent. South Univ. For. Technol.* **2016**, *36*, 59–64.

31. Ma, J.; Edmunds, W.M. Groundwater and lake evolution in the Badain Jaran Desert ecosystem, Inner Mongolia. *Hydrogeol. J.* **2006**, *14*, 1231–1243. [[CrossRef](#)]
32. Yuan, L.; Wu, S. *Groundwater System in Arid Area—Groundwater System on the West Side of Helan Mountain*; Geological Publishing House: Beijing, China, 1996.
33. Yang, Y.; Lu, Y.; Li, X.; Liang, X. Analysis of groundwater reservoir system in the piedmont of the west side of Helan Mountain. *J. Arid Land Resour. Environ.* **2017**, *31*, 62–67.
34. Li, P.-C.; Lu, Y.-D.; Wang, J.-K. *Study on the Bearing Capacity and Sustainable Utilization of Groundwater Resources in Alashan YaoBa Oasis*; Chang'an University: Xi'an, China, 2006.
35. Li, H.; Lu, Y.; Zheng, C.; Zhang, X. Seasonal and inter-annual variability of groundwater and their responses to climate change and human activities in arid and desert areas: A case study in Yaoba Oasis, Northwest China. *Water* **2020**, *12*, 303. [[CrossRef](#)]
36. Li, H.; Lu, Y.; Zheng, C.; Yang, M.; Li, S. Groundwater Level Prediction for the Arid Oasis of Northwest China Based on the Artificial Bee Colony Algorithm and a Back-propagation Neural Network with Double Hidden Layers. *Water* **2019**, *11*, 860. [[CrossRef](#)]
37. Cui, G.Q.; Lu, Y.D.; Zheng, C.; Liu, Z.H.; Sai, J.M. Relationship between Soil Salinization and Groundwater Hydration in Yaoba Oasis, Northwest China. *Water* **2019**, *11*, 175. [[CrossRef](#)]
38. Li, L. Comprehensive treatment plan for groundwater overdraft area in Alxa League. *Inn. Mong. Water Conserv.* **2018**, *38*, 54–55.
39. Fuoco, I.; Marini, L.; De Rosa, R.; Figoli, A.; Gabriele, B.; Apollaro, C. Use of reaction path modelling to investigate the evolution of water chemistry in shallow to deep crystalline aquifers with a special focus on fluoride. *Sci. Total Environ.* **2022**, *830*, 154566. [[CrossRef](#)]
40. Li, H.-H.; Lu, Y.-D.; Zhang, X.-Z.; Zheng, C. Analysis on Groundwater Dynamic Characteristics and Causes in Yao Ba Oasis. *Earth Sci.* **2015**, *4*, 241–246. [[CrossRef](#)]
41. Trabelsi, F.; Bel Hadj Ali, S. Exploring Machine Learning Models in Predicting Irrigation Groundwater Quality Indices for Effective Decision Making in Medjerda River Basin, Tunisia. *Sustainability* **2022**, *14*, 2341. [[CrossRef](#)]
42. Su, Y.H.; Zhu, G.F.; Feng, Q.; Li, Z.Z.; Zhang, F.P. Environmental isotopic and hydrochemical study of groundwater in the Ejina Basin, northwest China. *Environ. Geol.* **2009**, *58*, 601–614. [[CrossRef](#)]
43. Moreno-Merino, L.; Aguilera, H.; Román, A.d.l.l. Are bottled mineral waters and groundwater for human supply different? *Sci. Total Environ.* **2022**, *835*, 155554. [[CrossRef](#)]
44. Ikram, J.; Bachaer, A.; Moez, B.; Emma, B.; Salem, B. Contribution of GIS tools and statistical approaches to optimize the DRASTIC model for groundwater vulnerability assessment in arid and semi-arid regions: The case of Sidi Bouzid shallow aquifer. *Arab. J. Geosci.* **2022**, *15*, 974. [[CrossRef](#)]
45. Zhao, S.; Sun, J. Analysis on the Present Situation of Water Resources in Alxa Left Banner and Study on Countermeasures. *Inn. Mong. Water Conserv.* **2018**, *38*, 29–30.
46. Hasan, S.; Ali, M.A. Occurrence of manganese in groundwater of Bangladesh and its implications on safe water supply. *J. Civ. Eng.* **2010**, *38*, 121–128.
47. Fuoco, I.; Rosa, R.D.; Barca, D.; Figoli, A. Arsenic polluted waters: Application of geochemical modelling as a tool to understand the release and fate of the pollutant in crystalline aquifers. *J. Environ. Manag.* **2021**, *301*, 113796. [[CrossRef](#)] [[PubMed](#)]
48. GB/T 14848-93; Quality Standard for Ground Water. Geological Publishing House: Beijing, China, 2017.
49. Apollaro, C.; Curzio, D.D.; Fuoco, I.; Bucciante, A.; Dinelli, E.; Vespasiano, G.; Castrignanò, A.; Rusi, S.; Barca, D.; Figoli, A.; et al. A multivariate non-parametric approach for estimating probability of exceeding the local natural background level of arsenic in the aquifers of Calabria region (Southern Italy). *Sci. Total Environ.* **2022**, *806*, 150345. [[CrossRef](#)]
50. Pant, R.R.; Zhang, F.; Rehman, F.U.; Wang, G.X.; Ye, M.; Zeng, C.; Tang, H.D. Spatiotemporal variations of hydrogeochemistry and its controlling factors in the Gandaki River Basin, Central Himalaya Nepal. *Sci. Total Environ.* **2018**, *622*, 770–782. [[CrossRef](#)] [[PubMed](#)]
51. Cary, L.; Petelet-Giraud, E.; Bertrand, G.; Kloppmann, W.; Aquilina, L.; Martins, V.; Hirata, R.; Montenegro, S.; Pauwels, H.; Chatton, E.; et al. Origins and processes of groundwater salinization in the urban coastal aquifers of Recife (Pernambuco, Brazil): A multi-isotope approach. *Sci. Total Environ.* **2015**, *530–531*, 411–429. [[CrossRef](#)] [[PubMed](#)]
52. Appelo, C.A.J.; Postma, D. *Geochemistry, Groundwater and Pollution*; CRC Press: London, UK, 2005. [[CrossRef](#)]
53. Mangold, D.C.; Chin-Fu, T. A summary of subsurface hydrological and hydrochemical models. *Rev. Geophys.* **1991**, *29*, 51–79. [[CrossRef](#)]
54. Li, Z.; Yang, Q.; Yang, Y.; Ma, H.; Wang, H.; Luo, J.; Bian, J.; Martin, J.D. Isotopic and geochemical interpretation of groundwater under the influences of anthropogenic activities. *J. Hydrol.* **2019**, *576*, 685–697. [[CrossRef](#)]
55. Stuyfzand, P.J. Patterns in groundwater chemistry resulting from groundwater flow. *Hydrogeol. J.* **1999**, *7*, 15–27. [[CrossRef](#)]
56. Ogbozige, F.J.; Toko, M.A. Piper Trilinear and Gibbs Description of Groundwater Chemistry in Port Harcourt, Nigeria. *Appl. Sci. Eng. Prog.* **2020**, *13*, 362–369. [[CrossRef](#)]
57. Hounslow, A.W. *Water Quality Data: Analysis and Interpretation*; Lewis Publisher: Boca Raton, FL, USA, 1995.
58. Wang, W.R.; Chen, Y.P.; Wang, W.H.; Yang, Y.H.; Hou, Y.F.; Zhang, S.; Zhu, Z.Y. Assessing the Influences of Land Use Change on Groundwater Hydrochemistry in an Oasis-Desert Region of Central Asia. *Water* **2022**, *14*, 651. [[CrossRef](#)]

59. Hu, Q.L.; Yang, Y.H.; Han, S.M.; Yang, Y.M.; Ai, Z.P.; Wang, J.S.; Ma, F.Y. Identifying changes in irrigation return flow with gradually intensified water-saving technology using HYDRUS for regional water resources management. *Agric. Water Manag.* **2017**, *194*, 33–47. [[CrossRef](#)]
60. Wang, B.; Qiu, H.; Xu, Q.; Zheng, X.; Liu, G. The Mechanism of Groundwater Salinization and Its Control in the Yaoba Oasis, Inner Mongolia. *Acta Geol. Sin.* **2010**, *74*, 362–369. [[CrossRef](#)]
61. Plummer, L.N.; Busby, J.F.; Lee, R.W.; Hanshaw, B.B. Geochemical modeling of the Madison Aquifer in parts of Montana, Wyoming, and South Dakota. *Water Resour. Res.* **1990**, *26*, 1981–2014. [[CrossRef](#)]